ISSN 1674-1056
http://cpb.iphy.ac.cn
http://iopscience.iop.org/cpb
中国物理 B
Chinese Physics
中国物理 Chinese Physics B

Protection-against-water-attack determined difference between strengths of backbone hydrogen bonds in kinesin's neck zipper region

Jing-Yu Qin(覃静宇), Yi-Zhao Geng(耿轶钊), Gang Lü(吕刚), Qing Ji(纪青), Hai-Ping Fang(方海平)
Citation: Chin. Phys. B . 2018, 27(2): 028704. **doi:** 10.1088/1674-1056/27/2/028704

Journal homepage: http://cpb.iphy.ac.cn; http://iopscience.iop.org/cpb

What follows is a list of articles you may be interested in

Molecular dynamic simulation of the thermodynamic and kinetic properties of nucleotide base pair

Yu-Jie Wang(王宇杰), Zhen Wang(王珍), Yan-Li Wang(王晏莉), Wen-Bing Zhang(张文炳)
Chin. Phys. B . 2017, 26(12): 128705. **doi:** 10.1088/1674-1056/26/12/128705

Modulation of intra- and inter-sheet interactions in short peptide self-assembly by acetonitrile in aqueous solution

Li Deng(邓礼), Yurong Zhao(赵玉荣), Peng Zhou(周鹏), Hai Xu(徐海), Yanting Wang(王延颋)
Chin. Phys. B . 2016, 25(12): 128704. **doi:** 10.1088/1674-1056/25/12/128704

Dynamic instability of collective myosin II motors

Jin-Fang Li(李金芳), Zi-Qing Wang(汪自庆), Qi-Kun Li(李奇昆), Jian-Jun Xing(邢建军), Guo-Dong Wang(王国栋)
Chin. Phys. B . 2016, 25(11): 118701. **doi:** 10.1088/1674-1056/25/11/118701

Initial conformation of kinesin’s neck linker

Geng Yi-Zhao, Ji Qing, Liu Shu-Xia, Yan Shi-Wei
Chin. Phys. B . 2014, 23(10): 108701. **doi:** 10.1088/1674-1056/23/10/108701

SPECIAL TOPIC — Soft matter and biological physics

Protection-against-water-attack determined difference between strengths of backbone hydrogen bonds in kinesin's neck zipper region*

Jing-Yu Qin(覃静宇)[1,2], Yi-Zhao Geng(耿轶钊)[3,4], Gang Lü(吕刚)[5], Qing Ji(纪青)[3,4,6,†], and Hai-Ping Fang(方海平)[1,‡]

[1] *Division of Interfacial Water and Key Laboratory of Interfacial Physics and Technology, Shanghai Institute of Applied Physics, Chinese Academy of Sciences, Shanghai* 201800, *China*
[2] *University of Chinese Academy of Sciences, Beijing* 100049, *China*
[3] *Institute of Biophysics, Hebei University of Technology, Tianjin* 300401, *China*
[4] *School of Science, Hebei University of Technology, Tianjin* 300401, *China*
[5] *Mathematical and Physical Science School, North China Electric Power University, Baoding* 071003, *China*
[6] *State Key Laboratory of Theoretical Physics, Institute of Theoretical Physics, Chinese Academy of Sciences, Beijing* 100190, *China*

(Received 7 September 2017; revised manuscript received 3 November 2017; published online 5 January 2018)

Docking of the kinesin's neck linker (NL) to the motor domain is the key force-generation process of the kinesin. In this process, NL's $\beta 10$ portion forms four backbone hydrogen bonds (HBs) with the motor domain. These backbone hydrogen bonds show big differences in their effective strength. The origins of these strength differences are still unclear. Using molecular dynamics method, we investigate the stability of the backbone HBs in explicit water environment. We find that the strength differences of these backbone HBs mainly arise from their relationships with water molecules which are controlled by arranging the surrounding residue sidechains. The arrangement of the residues in the C-terminal part of $\beta 10$ results in the existence of the water-attack channels around the backbone HBs in this region. Along these channels the water molecules can directly attack the backbone HBs and make these HBs relatively weak. In contrast, the backbone HB at the N-terminus of $\beta 10$ is protected by the surrounding hydrophobic and hydrophilic residues which cooperate positively with the central backbone HB and make this HB highly strong. The intimate relationship between the effective strength of protein backbone HB and water revealed here should be considered when performing mechanical analysis for protein conformational changes.

Keywords: kinesin, neck linker, water

PACS: 87.16.Nn, 87.10.Tf, 87.15.hp **DOI:** 10.1088/1674-1056/27/2/028704

1. Introduction

Conventional kinesin[1] (kinesin-1, here is referred to as kinesin) is a highly processive motor protein, which effectively converts the chemical energy carried by adenosine triphosphate (ATP) into mechanical force and walks hundreds of steps along a microtubule with cargos.[2–5] Kinesin's neck linker (NL) docking to the motor domain is the key force generation step of kinesin.[6] The NL consists of $\sim$ 14 amino acids that connect kinesin's motor domain and coiled-coil stalk.[7] The C-terminal $\beta 10$ of NL docks to the motor domain through forming four backbone hydrogen bonds (HBs). These backbone HBs, though they are formed in the same way, show big differences in their effective strength.[8] To understand the docking mechanism of $\beta 10$, it is necessary to find out the origin of the strength difference among these backbone HBs at an amino acid level.

In kinesin walking cycle, NL undergoes a large conformational change from the undocked state to the docked state repeatedly (Fig. 1).[6,9] The NL consists of three parts, including the first three N-terminal amino acids (Lys325, Thr326 and Ile327 in 2KIN[10]), $\beta 9$ and $\beta 10$ (Fig. 1(a)).[11,12] These three parts of NL dock to the motor domain in three different ways. The first three amino acids dock to the motor domain through forming an extra turn structure, which is the initial step of the NL docking process driven by ATP binding induced motor head rotation and torsion.[11] The $\beta 9$ docks to the motor domain through forming a cover-neck bundle (CNB) structure with the N-terminal $\beta 0$ strand, which has a forward bending tendency.[12,13] In the docked state, $\beta 10$ forms four backbone HBs with the motor domain (Fig. 1(b)). In their work on the CNB mechanism of NL docking, Hwang *et al.*[12] performed MD simulations of the undocking process of NL and found

*Project supported by the National Natural Science Foundation of China (Grant No. 11605038) and the Open Project Program of State Key Laboratory of Theoretical Physics, Institute of Theoretical Physics, Chinese Academy of Sciences, China (Grant No. Y5KF211CJ1).

†Corresponding author. E-mail: jiqingch@hebut.edu.cn
‡Corresponding author. E-mail: fanghaiping@sinap.ac.cn

© 2018 Chinese Physical Society and IOP Publishing Ltd

that the backbone HBs at the C-terminal part of $\beta 10$ can be broken easily. However, the backbone HB at the N-terminus of $\beta 10$, the backbone HB between Asn334 and Gly77 (the ASN latch), is much stronger than other backbone HBs. They used ~ 450 pN force to break the ASN latch in their simulations with implicit water model. In one of our previous studies, we investigated the binding strength of NL with the motor domain by using MD simulations with explicit water model.[8] We found that the minimal unbinding force for the N-terminal ASN latch within tens of nanoseconds is 160 pN. In contrast, the backbone HBs at C-terminus of $\beta 10$ are unstable and can be broken even in the case without an unbinding force.

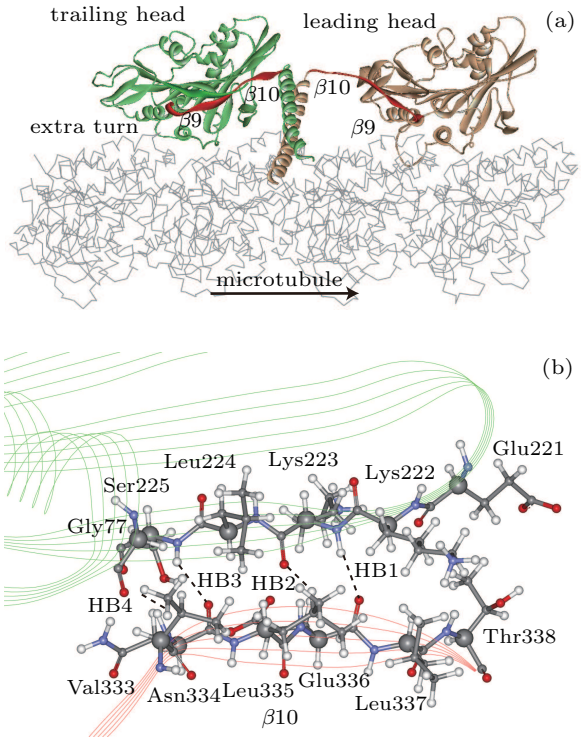


Fig. 1. (color online) Structure of kinesin motor domain and the backbone hydrogen bonds of the $\beta 10$ zipper. (a) Two motor heads and the neck coiled coil on microtubule. The neck linker (red) of the leading head is in the undocked state and that of the trailing head is in the docked state. (b) Definition of the four backbone HBs in the docked $\beta 10$ region. The HBs are indicated with broken lines. The oxygen atoms are shown in red balls, the hydrogen atoms in white, the nitrogen atoms in blue and α carbon atoms in bigger black balls.

The difference between the unbinding forces in the above two studies with implicit and explicit water models may be attributed to the difference in simulation times. However, another reason for the difference might be due to the way the role of water is described. In this work, we set up an MD model with kinesin motor head surrounded by explicit water molecules and investigate the origin of the strength difference of $\beta 10$'s backbone HBs. We find that the effective strength of a backbone HB is mainly determined by whether its hydrogen bonding sites could be attacked by water molecules. The high strength of the N-terminal ASN latch is achieved due to the perfect protection against water attack from both sides of the β-sheet and the C-terminal backbone HB has two water attack channels that make it rather weak. The water-dependence of the effective strength of protein backbone HBs must be taken into account when performing mechanical analysis for proteins.

2. Method

The MD simulations were performed by using NAMD (version 2.9)[14] with force field CHARMM.[15] Modeling and data analysis were performed with VMD (version 1.9.2).[16] The non-bonded Coulomb and van der Waals interactions were calculated with a cutoff using a switching function starting at a distance of 20 Å and reaching zero at 22 Å. The structural model for simulation is based on a crystal structure of rat kinesin (PDB ID: 2KIN).[10] The 2KIN's $\beta 7$ (the residues after Ala339), ADP and SO4 were deleted since they had little relation with interactions between $\beta 10$ and motor domain. Because L11 loop could not affect $\beta 10$-motor domain interaction, the missing part of L11 loop was ignored. The Val239 and Asn256 were directly connected in the modeling. The motor domain was surrounded by explicit water molecules and the spherical boundary condition was used. The water model is TIP3P.[17] To mimic the microtubule-bound state, we fixed the C_α atoms of Asn264, Ser267, Lys315, and Met319 in the simulation. The system was minimized to 30000 steps and the MD simulation took 40 ns. The system was simulated 11 times to perform statistical analysis. Molecular drawing was produced by using Discovery studio 3.5 visualizer.

3. Results

3.1. Four backbone HBs between kinesin's $\beta 10$ and motor domain showing big stability difference in NL docked state

A backbone HB in protein is formed between the backbone carbonyl oxygen and the backbone amide hydrogen. In the docked state, the $\beta 10$ portion of NL forms four backbone HBs with the motor domain, including HB1 (Glu336:O–Lys223:H), HB2 (Glu336:H–Lys223:O), HB3 (Asn334:O–Ser225:H), and HB4 (Asn334:H–Gly77:O) (Fig. 1(b)). The strengths of backbone HBs can be described by the bond length, i.e., the distances between the oxygen and hydrogen atoms, denoted as d_{HB1}, d_{HB2}, d_{HB3}, and d_{HB4}. Figure 2 shows the distance–time curves of the four HBs in one of our MD simulation trajectories (40 ns) for the docked NL (see Section 2). As seen, the four curves fluctuate with different amplitudes, indicating that the four backbone HBs have big stability differences in thermal environment. Taking 3 Å between hydrogen and oxygen atoms as the hydrogen bonding criterion, the bond stability can be quantified by calculating the bonding ratio over the entire trajectory ensemble (11 runs altogether, 40 ns each, see supporting information). The statistical result gives that the bonding ratios for HB1, HB2, HB3, and HB4

are 37%, 80%, 78%, and 97%, respectively. The big difference in the bonding ratio reflects that the four backbone HBs have quite different effective strengths, though they are formed in the same way. The N-terminal HB4 (the ASN latch) is highly stable while the C-terminal HB1 is rather weak, which is consistent with the previous findings.[8,12] The origins of the strength of these backbone HBs will be analyzed below.

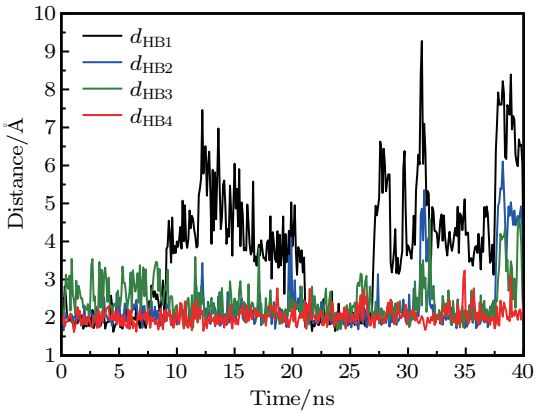


Fig. 2. (color online) Distance–time curves of the four backbone HB donor–acceptor distances in one typical MD trajectory with docked NL. HB4 is highly stable with d_{HB4} (red)< 3 Å. HB1 (black) is highly unstable. The regions where HB2 is broken (i.e., d_{HB2} (blue) > 3 Å) are always contained in the regions where HB1 is broken.

3.2. Water attacks along two water channels making the C-terminal backbone HB unstable

A detailed analysis of the trajectories shows that the instability of HB1 arises from water attacks. The HB1 is located at the C-terminus of β10. In Fig. 3, the distance–time curve of the distance between the hydrogen atom of a water molecule and the oxygen atom of HB1 (d_{EO-WH}) is depicted together with that of the donor–acceptor distance (d_{HB1}), which shows a typical water attack process. It is seen clearly that the HB1 is broken when the water molecule forms HB with the acceptor atom (oxygen) of HB1.

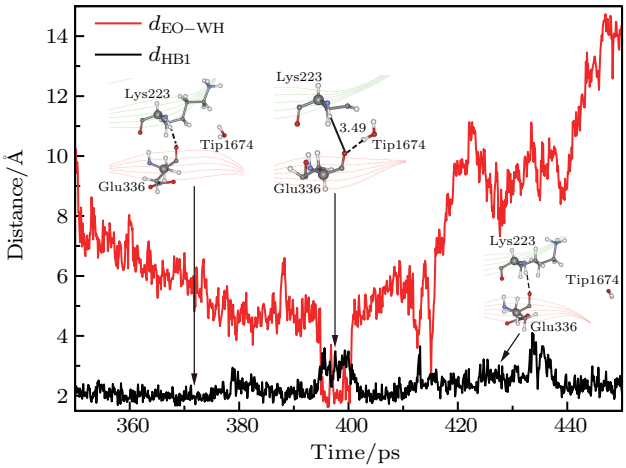


Fig. 3. (color online) HB1 breaking caused by water attack. The curve of d_{HB1} (black) shows a typical breaking event of HB1 ($d_{HB1} > 3$ Å) at around 400 ps, where the curve of the distance between the hydrogen atom of one water molecule and the oxygen atom of HB1 (red) shows a typical HB formation event ($d_{EO-WH} < 3$ Å). Three typical structures are shown in the three boxes.

The possible water attack region around the four HBs is divided into three sides, A, B, and C, respectively (as shown in Fig. 4). The structures of these three sides are different. On the A side of HB1 two hydrophobic residues (Leu335 and Leu337) and the aliphatic moiety of Lys222 form a compact group through hydrophobic interactions which effectively protect HB1 from water's attacking from this side (Fig. 5(a)). Four residues (Glu221, Lys223, Glu336, and Thr338) on the B side of HB1 form a channel for water attack (Fig. 5(b)). The average diameter of the water channel is ~ 4 Å (Fig. 5(b)), just large enough for the entrance of a water molecule (the diameter of a water molecule is ~ 2.8 Å). Analysis of the simulation trajectories shows that some breaking events of HB1 are caused by the attack of water molecule coming through this channel as shown in Fig. 5(b). On the C side of HB1, the backbone parts of Thr338 and Glu221 form another water channel (Fig. 5(c)). The water attack through this channel takes a different way. Thr338 and Glu221, whose locations are adjacent to HB1, expose their backbone HB sites to the water environment. In the crystal structure of kinesin (2KIN), there is a water bridge between these two residues instead of a backbone HB. In the dynamical trajectories, the water molecule, which forms a water bridge between Thr338 and Glu221, can sometimes form HB with the oxygen of Glu336 to break HB1. An event of water attack through this channel is shown in Fig. 5(c).

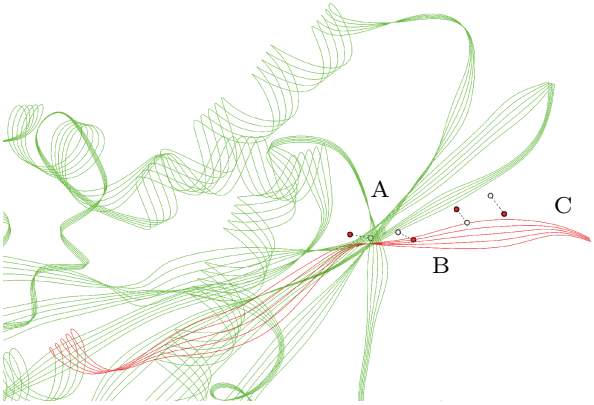


Fig. 4. (color online) Definitions of the three sides of β10 zipper. The upper region over the β-sheet formed by β10 and motor domain is defined as the A side, the lower region under the β-sheet the B side, and the side region the C side.

Glu336 and Lys223 form two backbone HBs, i.e., HB1 and HB2. The bonding ratio of HB2 is 80%, indicating that it is an effective HB. Structural analysis shows that there is a water channel formed by Lys223, Ser225, Asn334, and Glu336 at the B side of HB2 that allows direct water attack on this backbone HB. However, the water attack along this channel is barely effective due to the constraint from two adjacent backbone HBs (HB1 and HB3). The breaking of HB2 has a correlation with the status of HB1. As seen from the distance–time curves of d_{HB1} and d_{HB2} in Fig. 2, the periods of HB2 breaking

are always contained in the periods of HB1 breaking, indicating that HB2 breaking needs HB1 breaking as a necessary condition. When HB1 is broken, the C side of HB2 is exposed to the surrounding water and, hence, similar to the case of HB1, HB2 can be broken through water attack from both B and C sides.

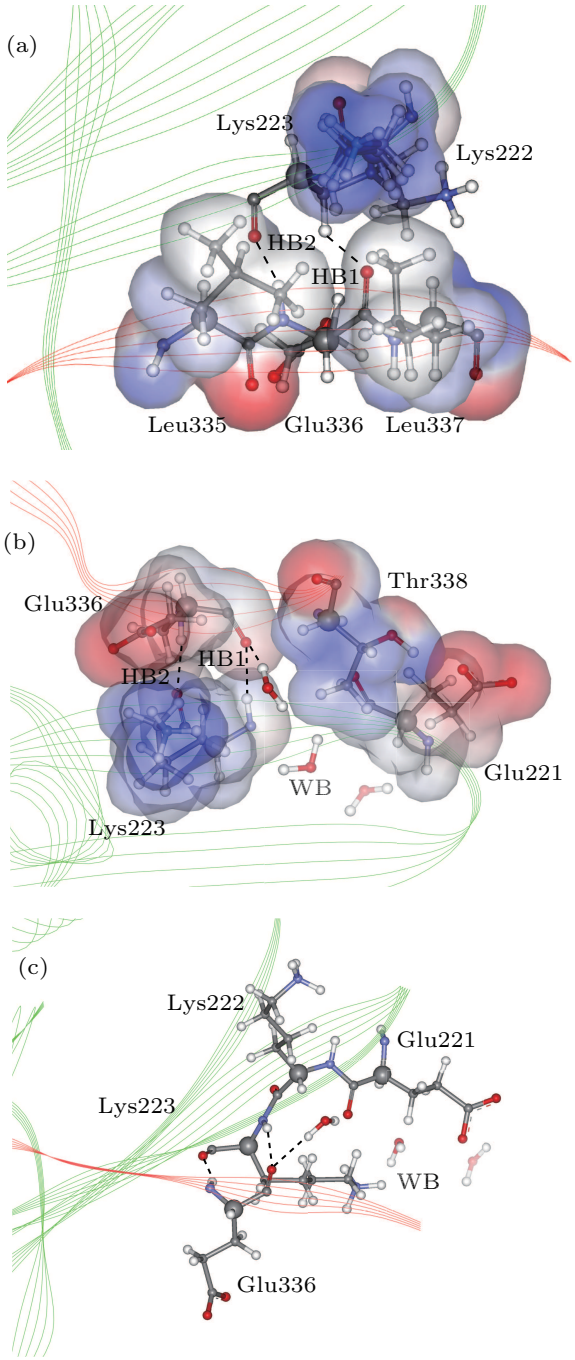


Fig. 5. (color online) Residue structures of the three sides around HB1. (a) A-side residue structure of HB1 formed by the sidechains of Lys222, Leu335, and Leu337. Two hydrophobic residues Leu335 and Leu337 form tight hydrophobic binding with the aliphatic stalk of Lys222 sidechain that effectively covers the A side of HB1 and prevents water attack on HB1 from this side. (b) Water attack channel at the B side of HB1. A water attack process is illustrated. (c) A C-side water attack on HB1. The water molecule becomes close to the acceptor oxygen atom of HB1 through forming a water bridge between the backbone oxygens of Glu221 and Glu336.

3.3. High strength of the backbone HB at the N-terminus of β10 arising from the cooperation among residues in this region which effectively prevent water's attacking

At the N-terminus of β10, Asn334 forms two backbone HBs with Ser225 (HB3) and Gly77 (HB4). The bonding ratio of HB4 is 97%, meaning that it is highly stable. However, the bonding ratio of HB3 is 78%, even lower than that of HB2 (80%). Figure 6 shows the conformation of the residues around HB3. As seen from Fig. 6(a), the hydrophobic group formed by Leu224, Val333, and Leu335 at the A side effectively protects HB3 from water attacking through this side. However, the residues (Ser225, Asn334, and Glu336) at the B side form an open structure that allows water molecules to attack HB3 easily (Fig. 6(b)). From the distance–time curves of HB3 in Fig. 2 and Fig. SI, it is seen that HB3 is not quite stable but the fluctuation of d_{HB3} is limited (generally smaller than 4 Å). The HB2 and HB4, adjacent to HB3, provide constraint on the distance fluctuation of HB3. Since HB4 is formed by Asn334 and Gly77 at the C-terminus of the helix β1, the constraint from HB4 is not so strong as that from HB2 located on the same β-sheet with HB3.

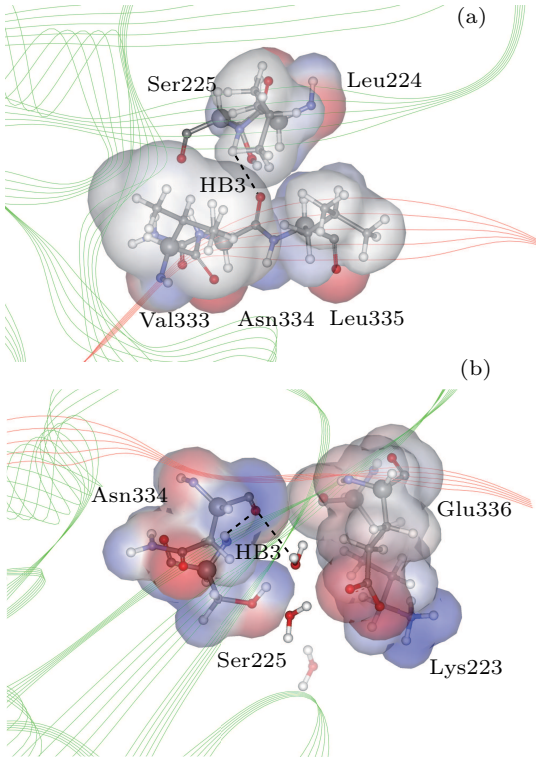


Fig. 6. (color online) Residue structures of the A and B sides of HB3. (a) Hydrophobic cover at A side of HB3 formed by Leu224, Val333, and Leu335. (b) Open water attack channel at B side of HB3 that allows water molecule to attack HB3 easily.

The HB4 is the central HB of the ASN latch which has a high effective strength. In the unbinding case,[11,12] ASN latch shows strong resistance to the unbinding force. The high stability of ASN latch is achieved through the cooperation of the residues arranged exquisitely (Fig. 7). At the

A side of HB4, three typical hydrophobic residues Leu224, Val333, Leu335 and an aromatic residue TYR78 bind tightly through hydrophobic interaction. These residues effectively protect HB4 from water attacking (Fig. 7(a)). The hydrophobic binding of these hydrophobic residues also makes a contribution to the high strength of ASN latch. At B side of HB4, the two residues (Ser225 and Asn334) with multi-HB sites cover the bonding region of HB4 (Fig. 7(b)). This special structure effectively protects HB4 through forming HBs with water molecules. When forming HBs with these two residues, water molecules cannot further enter into the HB4 region.

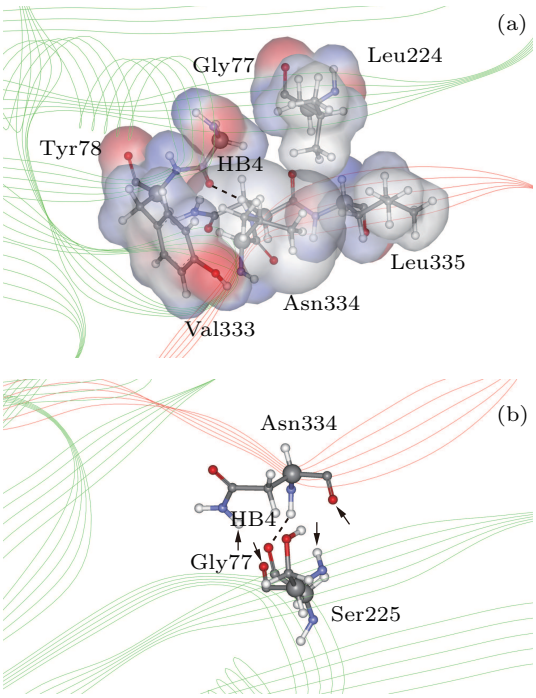


Fig. 7. (color online) Two-sided protection of HB4 from water attacking. (a) Hydrophobic cover at A side of HB4 formed by Tyr78, Leu224, Val333, and Leu335. (b) Hydrogen bonding sites (black arrows) around HB4 at B side that prevents water molecules attacking the donor and acceptor of HB4 directly.

4. Discussion

Kinesin is a molecular walking device working in water environment. The movement of kinesin is achieved through a series of conformational changes, in which many nonbonding interactions, especially backbone HBs, are formed or broken. The result of this work shows that water is highly important in controlling the effective strength of backbone HBs. This knowledge must be taken into account in understanding the design principle of kinesin.

4.1. Highly water-dependent effective strength of backbone HBs

The average bond energy of a protein backbone HB is ~ 25 kJ/mol. Taking the force-range of a HB to be ~ 1 Å, the average force of a backbone HB is ~ 410 pN. In this calculation, the water influence is not taken into account, i.e., the direct breaking of an HB in the absence of water needs a force > 400 pN. The result of this work, however, shows that the effective strength of an HB is highly water-dependent. Due to the presence of two water attack channels, HB1 is easily attacked by water molecules and its breaking can even occur without any force. Therefore, the bonding ratio of HB1 is quite low (37%). The water channel of HB3 is an open structure that allows water molecules to attack HB3 more easily than to attack HB2. This thus makes the bonding ratio of HB3 (78%) lower than that of HB2 (80%). The HB4 (the central backbone HB of the ASN latch) is perfectly protected from water attacking so that its bonding ratio (97%) is close to 100%. These bonding ratio differences among the backbone HBs are consistent with the unbinding force differences among the backbone HBs revealed in Hwang *et al.*'s work and one of our previous works.[8,12] It is found that the unbinding force for HB4 (the ASN latch) is much stronger than for the other three and the unbinding force for HB1 is rather weak.

The backbone HBs play a major role in the mechanical behavior of proteins. Since the effective strength of backbone HBs is highly water-dependent, this water dependence must be taken into account in the analysis of the mechanical behavior of proteins. Then, how to quantitatively describe the water dependence of backbone HBs becomes an unavoidable question. Due to the complicity concerning the properties of the sidechains of the related residues and their relationship, this question is still a challenging open question.

4.2. Arrangement of the backbone HBs with gradient strength ensuring efficient docking of NL

The NL docking is the key force-generation process of kinesin, which is accomplished in three steps including the initiation step of the first three residues forming an extra turn, the docking of $\beta 9$ via the CNB mechanism, and the docking of $\beta 10$. Unlike the first two steps, the docking of $\beta 10$ takes a zipper mechanism, i.e., the four backbone HBs form one after another automatically. As shown in the above section, neighboring backbone HBs have close correlations. Formation of one backbone HB will largely promote the formation of the neighboring one. Hydrogen bonds are of short-range interactions with force-range within 3 Å. Once a backbone HB is formed, the donor and acceptor atoms of the neighboring HB are restricted in a small space so that the formation probability of the neighboring HB is greatly increased. A backbone HB might be attacked by water molecules from all possible channels. Formation of one backbone HB will lessen the water attack on the neighboring HB. Evidently, to ensure efficient docking of NL, the formation of the initial backbone HB of the zipper is crucial. This HB should be strong and stable so that zippering up process could go on efficiently. In the design of kinesin, the initial backbone HB of the $\beta 10$ zipper is HB4. As shown above, HB4 is the strongest and stablest backbone HB of the $\beta 10$ zipper. Once HB4 is formed, it is hard to break. In one of our previous works,[8] we find that more than one-third

of the work done in unbinding the entire NL is for deposition in the process of opening the ASN latch. The design with HB4 serving as the first HB of the $\beta 10$ zipper ensures the efficient docking of NL.

It should be pointed out that the high strength of HB4 does not mean that its spontaneous formation could take place easily. The simulation work with implicit water by Hwang *et al.*[12] shows that CNB bends toward the binding pocket nearly deterministically, but the docking of $\beta 10$ from an undocked state, especially the latching of the ASN latch, was not observed within the simulation time. In our simulation with explicit water, we capture the spontaneous docking of $\beta 10$ starting from a CNB docked and $\beta 10$ undocked structure. Figure 8 shows the details of the $\beta 10$ docking process within 25 ns. As seen from Fig. 8(a), the docking process occurs in four steps. At the beginning, the four distances between the backbone HB binding sites are all much larger than 3 Å, indicating that $\beta 10$ is totally unbound, see Fig. 8(b). In the second step, $\beta 10$ enters into a metastable state with d_{HB4} fluctuating around 4 Å. This metastable state is obtained mainly through forming two water bridges between NL and motor domain. The first water bridge is formed between the backbone parts of Asn79 and Ser332 and the second water bridge is formed between the acceptor and donor sites of HB4 (Fig. 8(c)). In the third step, HB4 is stably formed while the other three backbone HBs are still open. One must be quite interested in what happens between the second and third step. The intermediate state with $d_{\mathrm{HB4}} = 3.21$ Å is shown in Fig. 8(d). As seen, two standard water bridges are found to be along the two sides of HB4 and finally form HB4. The first water bridge is formed via the same water molecule as that in Fig. 8(c), indicating that this water bridge is rather stable. In the crystal structure of 2KIN,[10] this water molecule is retained as a bound water molecule and plays an important constructive role.[18] The second water bridge is found through a water molecule different from that in Fig. 8(c). It is worth noting that this water bridge is formed between the sidechain of Asn334 and the acceptor site of HB4 on Gly77 rather than between the donor and acceptor site of HB4 as in the case of Fig. 8(c). Formation of this water bridge effectively promotes the formation of HB4, while the water bridge directly formed between the donor and acceptor site of HB4 inhibits the HB4 from forming. In the fourth step, the next three backbone HBs are normally formed with HB1 weaker than the others.

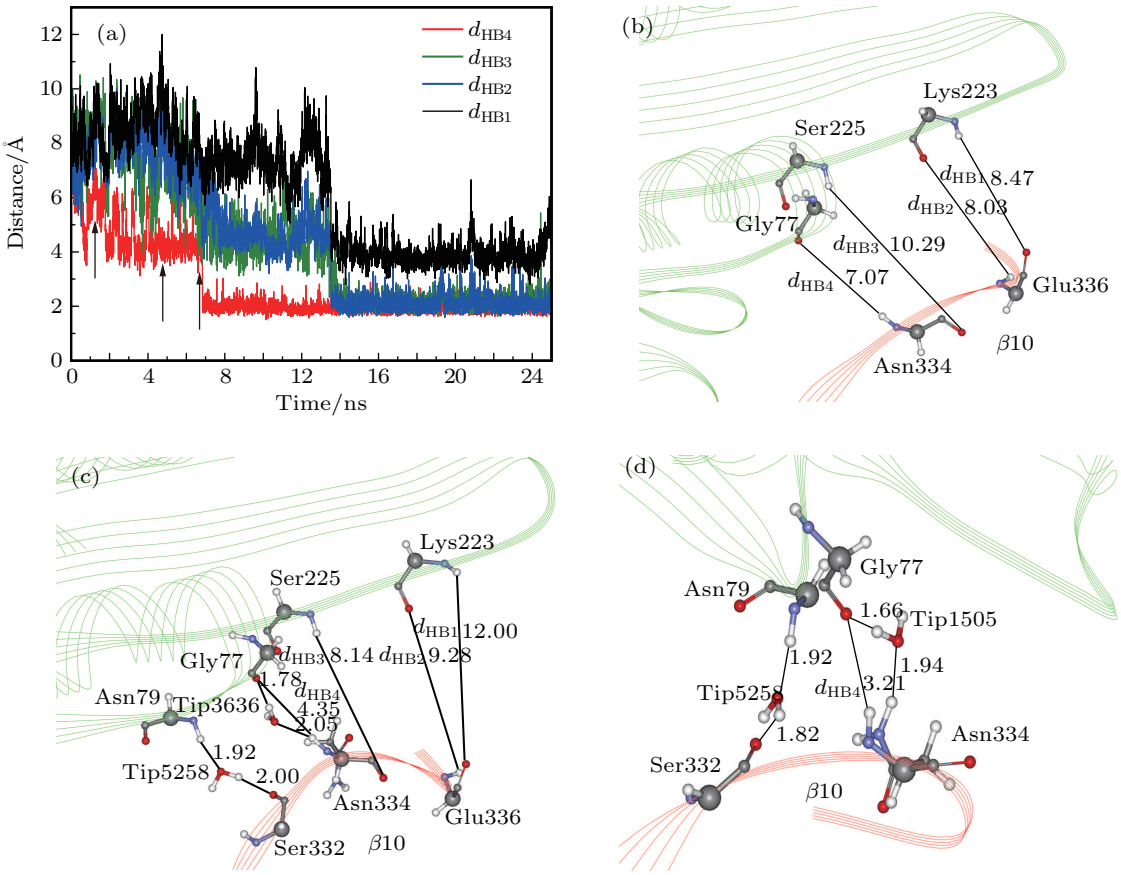


Fig. 8. (color online) Docking process of $\beta 10$. (a) Distance–time curves of d_{HB1}, d_{HB2}, d_{HB3}, and d_{HB4} in the $\beta 10$ docking process with four steps. Three black arrows indicate the positions of three typical conformations shown in panels (b), (c) and (d). (b) Conformation of unbound $\beta 10$ at ~ 1.5 ns (first arrow) in the first step. The distances are all in unit [Å]. (c) Conformation of $\beta 10$ in the metastable state at ~ 4.8 ns (second arrow) in the second step. Two water bridges are formed between NL and the motor domain, which make a key contribution to the formation of the metastable state. (d) Conformation of $\beta 10$ in the intermediate state between the second and third step at ~ 6.7 ns (third arrow). Two water bridges are formed with the second one formed between the sidechain of Asn334 and the acceptor site of HB4 on Gly77 rather than between the donor and acceptor site of HB4 as in the case of panel (c).

Life arises from water. The intimate relationship between protein backbone hydrogen bonds and water as revealed here shows that the protein properties are determined together with water. Therefore, to obtain a real understanding of protein behavior, one must figure out those protein–water interaction details.

Acknowledgement

The authors would like to thank the Computer Network Information Center of Chinese Academy of Sciences and the Shanghai Supercomputer Center of China for computing service.

Supporting information

Distance–time curves of d_{HB1}, d_{HB2}, d_{HB3}, and d_{HB4} in 40-ns simulations of 11 runs.

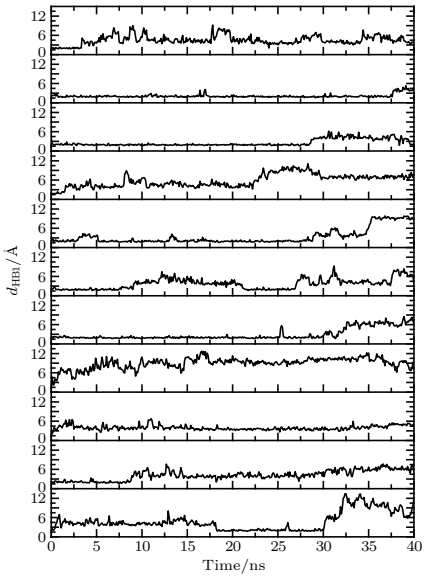


Fig. S1. Distance–time curves of d_{HB1} in 11 MD simulations.

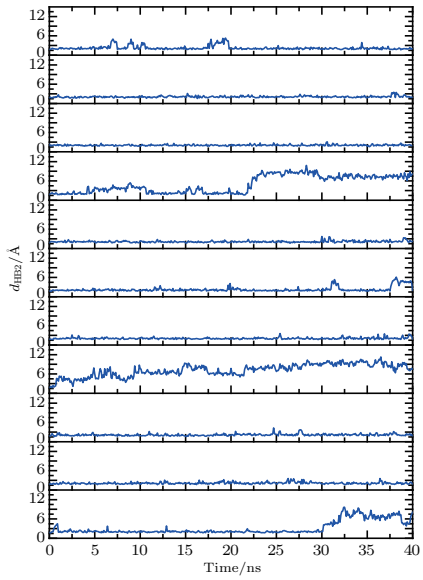


Fig. S2. (color online) Distance–time curves of d_{HB2} in 11 MD simulations.

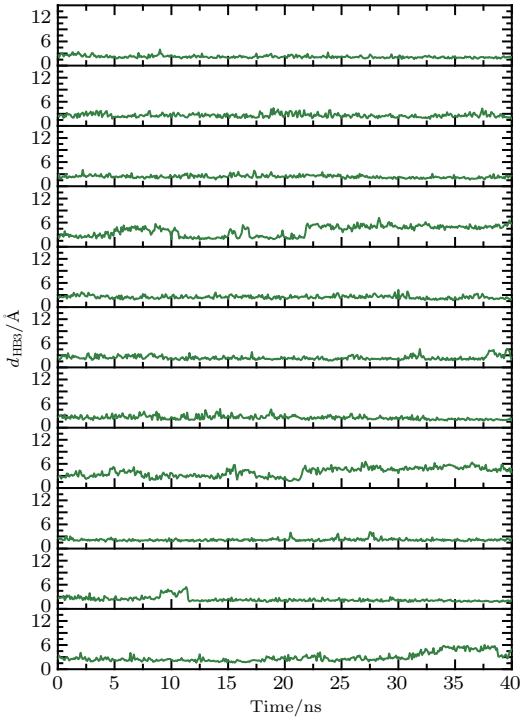


Fig. S3. (color online) Distance–time curves of d_{HB3} in 11 MD simulations.

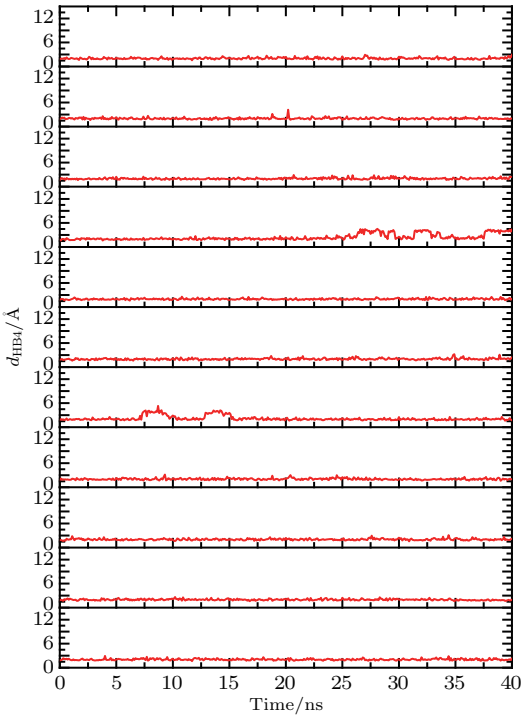


Fig. S4. (color online) Distance–time curves of d_{HB4} in 11 MD simulations.

References

[1] Lawrence C J, Dawe R K, Christie K R, Cleveland D W, Dawson S C, Endow S A, Goldstein L S, Goodson H V, Hirokawa N, Howard J, Malmberg R L, McIntosh J R, Miki H, Mitchison T J, Okada Y, Reddy A S, Saxton W M, Schliwa M, Scholey J M, Vale R D, Walczak C E and Wordeman L 2004 *J. Cell Biol.* **167** 19
[2] Block S M 2007 *Biophys. J.* **92** 2986
[3] Hirokawa N and Noda Y 2008 *Physiol. Rev.* **88** 1089
[4] Sindelar C V 2011 *Biophys. Rev.* **3** 85
[5] Vale R D and Milligan R A 2000 *Science* **288** 88

[6] Rice S, Lin A W, Safer D, Hart C L, Naber N, Carragher B O, Cain S M, Pechatnikova E, Wilson-Kubalek E M, Whittaker M, Pate E, Cooke R, Taylor E W, Milligan R A and Vale R D 1999 *Nature* **402** 778
[7] Hariharan V and Hancock W 2009 *Cell Mol. Bioeng.* **2** 177
[8] Geng Y Z, Li T, Ji Q and Yan S W 2014 *Cell Mol. Bioeng.* **7** 99
[9] Asenjo A B, Weinberg Y and Sosa H 2006 *Nature Structural and Molecular Biology* **13** 648
[10] Sack S, Mäuller J, Marx A, Thormäahlen M, Mandelkow E M, Brady S T and Mandelkow E 1997 *Biochemistry* **36** 16155
[11] Geng Y Z, Ji Q Liu S X and Yan S W 2014 *Chin. Phys. B* **23** 108701
[12] Hwang W, Lang M J and Karplus M 2008 *Structure* **16** 62
[13] Khalil A S, Appleyard D C, Labno A K, Georges A, Karplus M, Belcher A M, Hwang W and Lang M J 2008 *Proc. Natl. Acad. Sci. USA* **105** 19247
[14] Phillips J C, Braun R, Wang W, Gumbart J, Tajkhorshid E, Villa E, Chipot C, Skeel R D, Kal?e L and Schulten K 2005 *J. Comput. Chem.* **26** 1781
[15] MacKerell A D, Bashford D, Bellott, Dunbrake R L, Evenseck J D, Field M J, Fischer S, Gao J, Guo H, Ha S, Joseph-MaCarthy D, Kuchnir L, Kuczera K, Lau F T K, Mattos C, Michnick S, Ngo T, Nyuyen D T, Prodhom B, Reiher W E, Roux B, Schlenkrich M, Smith J C, Stote R, Straub J, Watanabe M, Wirkiewicz-Kuczera J, Yin D and Karplus M 1998 *J. Phys. Chem.* **102** 3586
[16] Humphrey W, Dalke A and Schulten K 1996 *J. Mol. Graphics* **14** 33
[17] Jorgensen W L, Chandrasekhar J, Madura J D, Impey R W and Klein M L 1983 *J. Chem. Phys.* **79** 926
[18] Huang Y B, Pan Z, Zhang H, An L, Kong D X, and Ji Q 2009 *Chin. Phys. Lett.* **26** 078701